Materials Science in Semiconductor Processing 16 (2013) 1957–1963

Contents lists available at ScienceDirect

Materials Science in Semiconductor Processing

journal homepage: www.elsevier.com/locate/mssp

Characteristics of Ga-doped ZnO films deposited by pulsed DC magnetron sputtering at low temperature

Kyung-Jun Ahn [a], Sanghun Lee [b], Won-Jeong Kim [c], Geun Young Yeom [a], Woong Lee [b,*]

[a] Department of Advanced Materials Science and Engineering, Sungkyunkwan University, 300 Cheoncheon-dong, Suwon, Gyeonggi 440-746, Republic of Korea
[b] School of Nano and Advanced Materials Engineering, Changwon National University, 9 Sarim-dong, Changwon, Gyeongnam 641-773, Republic of Korea
[c] Department of Physics, Changwon National University, 9 Sarim-dong, Changwon, Gyeongnam 641-773, Republic of Korea

ARTICLE INFO

Available online 15 August 2013

Keywords:
Transparent conductive oxide
ZnO
Ga-doping
Pulsed DC magnetron sputtering
Absorption spectra
X-ray photoelectron spectroscopy

ABSTRACT

Characteristics of Ga-doped ZnO (GZO) transparent conductive oxide films have been investigated based on the absorption behavior and chemical states of dopant Ga in the film. GZO samples were prepared by pulsed DC magnetron sputtering at 423 K by varying the sputtering power from 0.6 to 2.4 kW and the Ga_2O_3 concentration in the targets from 0.6 to 5.7 wt%. Absorption spectra of the GZO films in the visible to ultraviolet range were characterized by long absorption tails and shoulders near the absorption edges indicating the presence of impurity states or bands that overlap with the conduction band. X-ray photoelectron spectroscopy and X-ray diffraction revealed that substantial portion of the dopant exists as finely dispersed or amorphous metallic Ga and oxide of Ga, which would be related to the formation of the impurity bands or states, especially in the samples with lower Ga content. Presence of these species is correlated to the limited doping efficiency observed in the GZO films.

1. Introduction

Demands for transparent conductive oxides (TCOs) are growing due to the recent developments in information technology. Devices such as light emitting diodes and flat panel displays typically employ tin-doped indium oxide (ITO) for transparent electrodes. ITO has many desirable properties such as low electrical resistivity, high optical transmittance in the visible wavelength range, ease of wide-area deposition via simple techniques like sputtering, etc. [1]. However, shortage of the precious metal indium [2,3] and technical problems such as poor mechanical flexibility [4] and instability under hydrogen plasma ambient [5] have stimulated efforts to develop ITO substitutes. Among many candidates, a wide-bandgap compound semiconductor ZnO is regarded as promising material due to the abundance of raw materials, nontoxicity, and chemical stability [2–3,6–8]. In order to decrease electrical resistivity, ZnO are doped with B, Al, Ga, In, and F, among which Al has been widely used for the dopant. Instead of Al, Ga can also be used. In the case of Ga-doped ZnO (GZO), Ga–O bond length of 1.92 Å is comparable to the Zn–O bond length of 1.97 Å [9] and therefore it is expected that the TCO would suffer less structural deformation during doping.

For the deposition of conductive GZO films, numerous thin film deposition techniques have been employed. Recently, pulsed DC magnetrons sputtering (PDCMS), which incorporates advantageous features of radio frequency (RF)

* Corresponding author. Tel.: +82 55 213 3697; fax: +82 55 261 7017.
E-mail addresses: woonglee@changwon.ac.kr, cwl10001@hanmail.net (W. Lee).

1369-8001/$ - see front matter © 2013 Elsevier Ltd. All rights reserved.
http://dx.doi.org/10.1016/j.mssp.2013.07.026

and DC systems [10,11], has been introduced. Advantages of PDCMS include high sputtering power in the range of few kW with high plasma density, long-term process stability with arc prevention, enhanced dynamic deposition rate enabling preparation of relatively defect-free films, etc [12–15]. Although these advantages enable large-area deposition of high-quality oxide films at high deposition rate, relatively few works are available on the deposition of GZO films by PDCMS. In our previous works, it was observed that electrical properties of GZO films deposited by PDCMS can be improved by combining higher Ga content in the sputtering target, higher deposition temperature, and higher sputtering power [16,17]. However, it was also observed that doping efficiency represented by relative concentrations of carrier electron with respect to the donor concentrations is somewhat limited. In order to further illuminate this aspect, spectroscopic analyses have been carried out on the GZO films deposited under various combinations of sputtering power and target composition in this study.

2. Experimental details

Ga-doped ZnO TCO films were deposited on glass substrates (Corning Eagle 2000) by pulsed DC magnetron sputtering (PDCMS) in Ar atmosphere at the working pressure of 0.67 Pa (base pressure was 3.0×10^{-4} Pa). Three square-shape ZnO ceramic targets (400×400 mm) containing 0.6, 3.0, and 5.7 wt% of Ga_2O_3 were used as the sources. For each target composition, three sputtering power conditions of 0.6, 1.2, 2.4 kW were applied to prepare nine batches of TCO samples while the substrate temperature was fixed at 423 K. Distance between the target and the substrate was fixed at 160 mm. The GZO

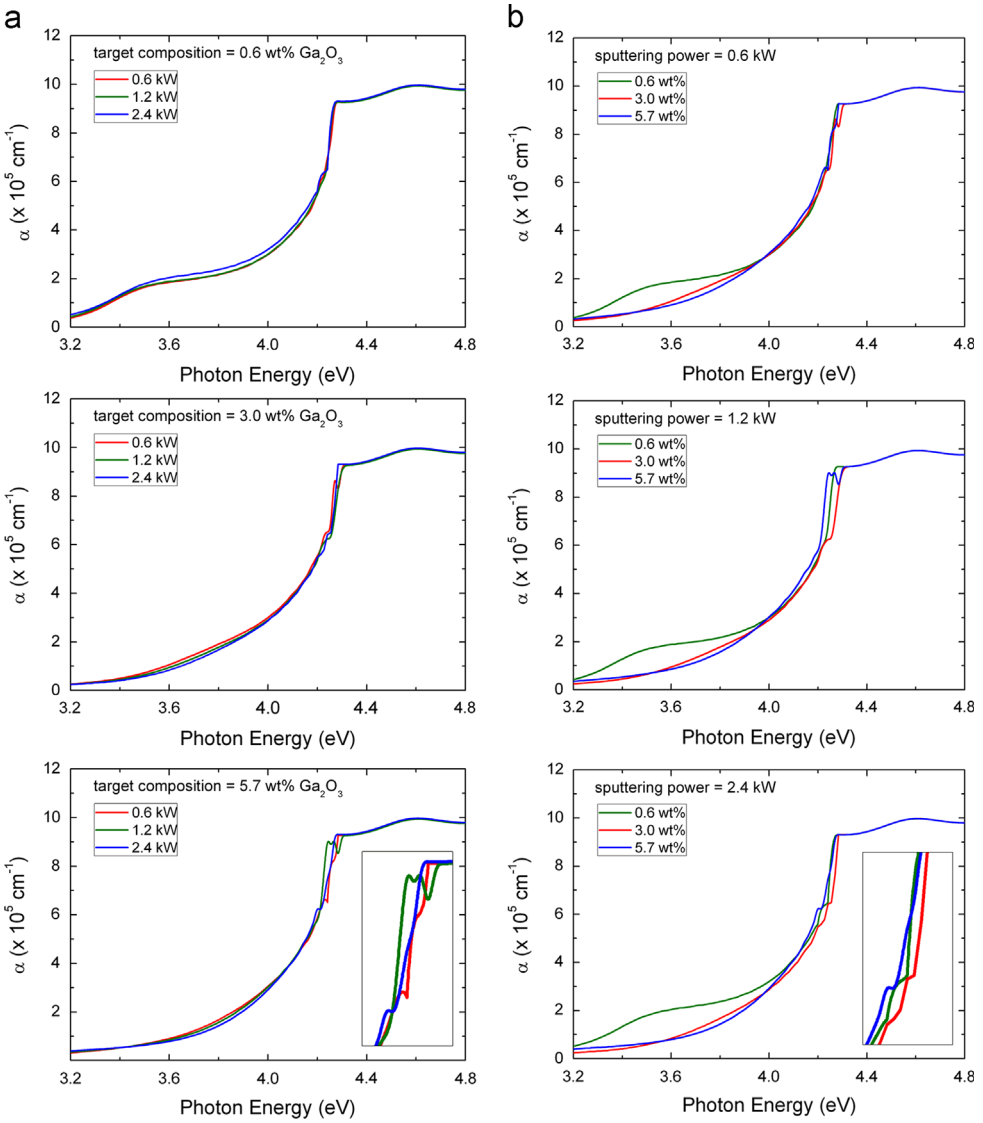

Fig. 1. Changes in the absorption spectra of the GZO films with varying deposition conditions: (a) spectra for various sputtering powers with fixed target compositions; (b) spectra for various target compositions with fixed sputtering powers.

films were deposited to the thickness of about 100 nm by controlling the deposition time based on the deposition rates calibrated from the relations between film thicknesses measured using a high resolution surface profiler having the resolution of 1 Å (α-step, AMBIOS Technology XP-1) and various sputtering times for each sputtering power. Pulse frequency was fixed at 50 kHz with the duty cycle of 72%, which gives the pulse factor of 14.4 μs. Absorption behaviors of the films were measured using a UV–vis spectrometer (JASCO, V-570) in the wavelength range of 200–800 nm. Chemical roles of the dopant Ga in the GZO films were analyzed using x-ray photoelectron spectroscopy in high vacuum (XPS, AXIS NOVA) and crystallinity of the films was analyzed by x-ray diffraction (XRD) in θ–2θ scan mode using a Ni-filtered Cu $K\alpha_1$ source (Philips X'pert MPD 3040). Concentration of carrier electrons in the GZO films were measured by a van der Pauw Hall method (Bridge Technology, Ecopia HMS-3000 Hall Measurement System) at room temperature with the applied magnetic field of 0.55 T in a dark condition.

3. Results and discussion

Total optical transmittances of the GZO/glass samples in the visible spectrum range were above 80% regardless of the deposition conditions satisfying the requirement for transparent electrode. However, the absorption behaviors were somewhat dependent on the deposition conditions. In Fig. 1, absorption coefficients (α's) are plotted against the photon energy of the incident lights. These absorption spectra are characterized by the large tails and shoulders near the absorption edges. For the fixed target composition, the overall shapes of the tails are not significantly affected by the sputtering power as seen in Fig. 1(a). Meanwhile, when the target composition was 5.7 wt% Ga_2O_3, shoulders are slightly more pronounced at lower sputtering powers as seen in the inset. When the target composition is varied (sputtering power is fixed), the absorption curves for the 0.6 wt% samples in Fig. 1(b) are distinguished by a large step-like tails at the incident photon energy of about 3.5–4.0 eV (λ=310–350 nm). In addition, shoulders at about 4.2–4.3 eV (λ=288–295 nm), which are common in all the absorption spectra, become slightly more noticeable with decreasing Ga_2O_3 concentration in the target when higher sputtering power is applied (see the inset). Shoulders and tails near the absorption edges are known to originate from the transition between the valence band and impurity states [18]. In this context, existence of large absorption tails and shoulders indicate that some impurities are incorporated in the GZO films which form impurity bands or states at energy levels near the bottom of the conduction band of ZnO. Such impurity states or bands (especially near the conduction band edge) seem to be more pronounced when Ga_2O_3 concentration in the sputtering target is lower.

Fig. 2 shows the Tauc plots for the GZO films deposited under various conditions. Optical bandgaps of the GZO films can be estimated from the absorption edges via the Tauc equation [19]

$$\alpha h\nu = A(h\nu - E_g)^n \quad (1)$$

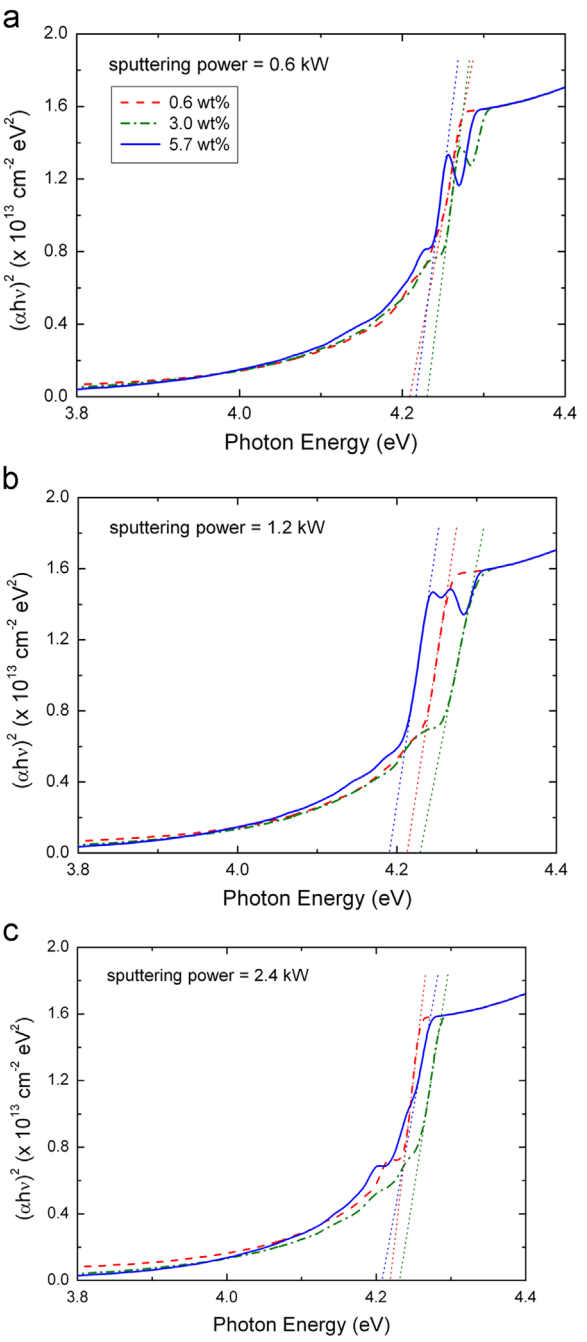

Fig. 2. Tauc plots for the GZO films deposited with various combinations of target composition and sputtering power.

where α is the absorption coefficient, h is the Planck constant, ν is the frequency of incident light, A is a constant, E_g is the optical bandgap, and the exponent n is taken to be 0.5 for direct gap semiconductors. In Fig. 2, optical bandgaps, taken from the intercepts of the tangent lines with the wavelength axis, vary slightly between 4.19 and 4.23 eV with no distinctive dependence on the deposition conditions. Incidentally, Table 1 shows that there are substantial differences in the concentration of carrier electrons in the GZO films depending on the deposition

Table 1
Changes in the carrier concentration ($\times 10^{20}$ cm^{-3}) of the GZO films with varying target compositions and sputtering powers. Error ranges reflect uncertainties in the thickness of the GZO films which is about 5%.

Target composition (wt% Ga_2O_3)		0.6	3.0	5.7
Sputtering power (kW)	0.6	0.399 ± 0.021	2.47 ± 0.13	4.15 ± 0.24
	1.2	0.388 ± 0.020	3.13 ± 0.16	5.00 ± 0.27
	2.4	0.520 ± 0.028	4.11 ± 0.21	6.77 ± 0.40

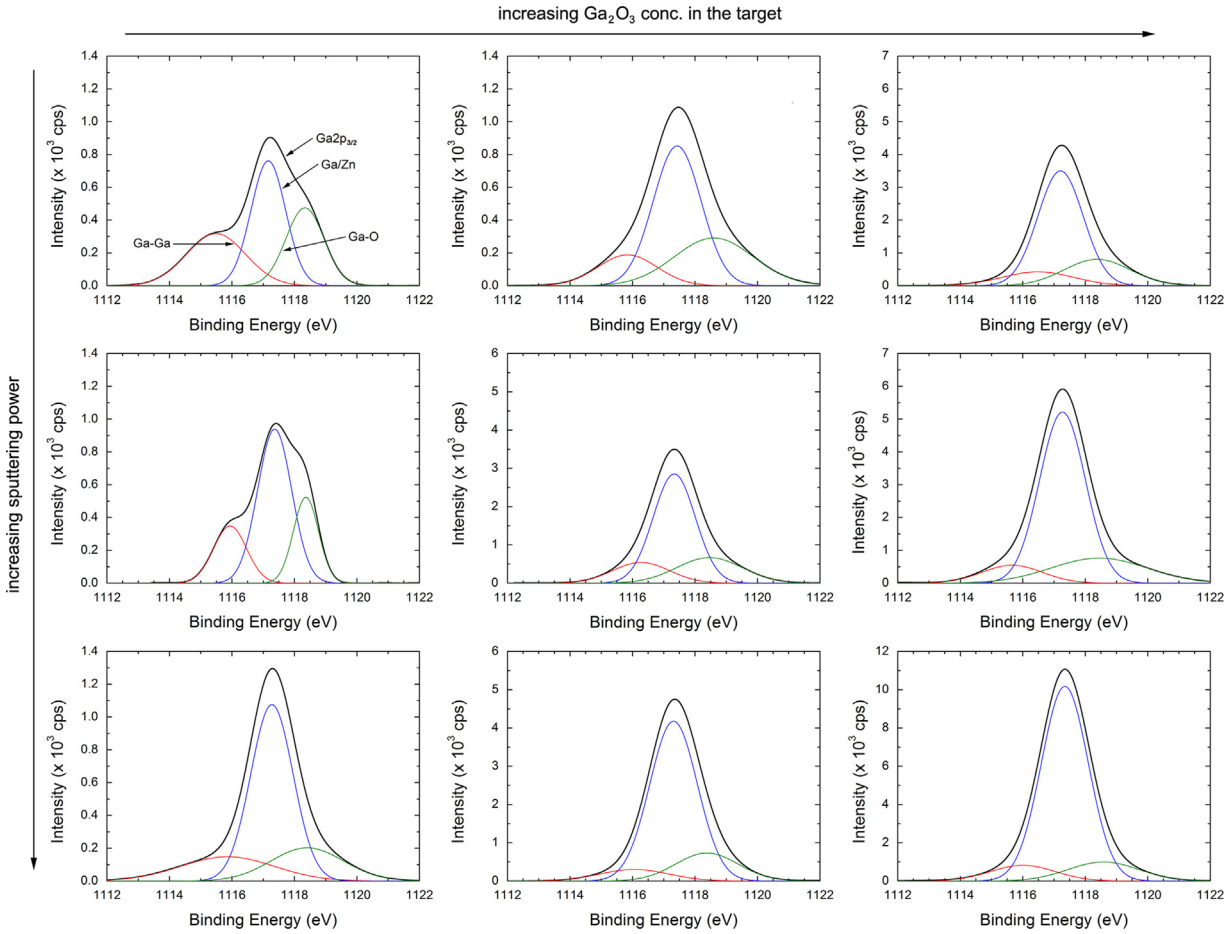

Fig. 3. Deconvoluted XPS spectra for the Ga $2p_{3/2}$ states obtained from the GZO films deposited under various deposition conditions. Note that the intensities are in different scales.

conditions, which may cause Burstein–Moss shift [20] in the optical bandgaps. Since Burstein–Moss shift is not observed in Fig. 2, it is presumed that the formation of the empty defect states or bands near the bottom of the conduction band (about 4.2 eV above the valence band maximum) as mentioned above is responsible for such composition-independent changes in optical bandgaps.

Optical properties of the GZO films described above suggest that substantial amount of impurities are incorporated into the GZO films during the deposition. Since GZO films were deposited using ZnO targets having various concentrations of Ga_2O_3, it is expected that Ga and/or its oxide(s) could be the primary sources of impurities. Hence, chemical states of Ga in GZO films were investigated using XPS peaks for Ga $2p_{3/2}$ states shown in Fig. 3. In Fig. 3, intensities of Ga $2p_{3/2}$ peaks increase with increasing Ga_2O_3 concentration in the target and also with higher sputtering power. Non-Gaussian shapes of these Ga $2p_{3/2}$ peaks suggest that they can be decomposed into subpeaks as shown in the figure. The subpeaks in Fig. 3 denoted as Ga–Ga (at 1115.7 eV), Ga/Zn (at 1117.3 eV), and Ga–O (at 1118.3 eV) are attributed to metallic gallium, Ga^{3+} ion substituting Zn^{2+} ion in ZnO lattice, and Ga^{3+} ion in oxide phase, respectively [21,22]. Presence of the metallic Ga and oxide peaks indicates that not all Ga have substituted lattice Zn to function as the dopant even when the target contains very low Ga_2O_3 concentration of 0.6 wt%.

Relative intensities of the subpeaks with respect to the intensity of the main peak as area fractions are summarized for various target compositions and sputtering powers in Fig. 4. It is seen that the relative intensity of the Ga/Zn peaks increases with increasing Ga_2O_3 concentration in the target and with higher sputtering power. This accompanies a decrease in the relative intensities of Ga–Ga and Ga–O subpeaks with increasing Ga_2O_3 content and sputtering power. These observations indicate that substantial portion of Ga can exist in the GZO films in metallic form (elemental Ga) and in oxide form without substituting the lattice Zn^{2+} ions regardless of deposition conditions.

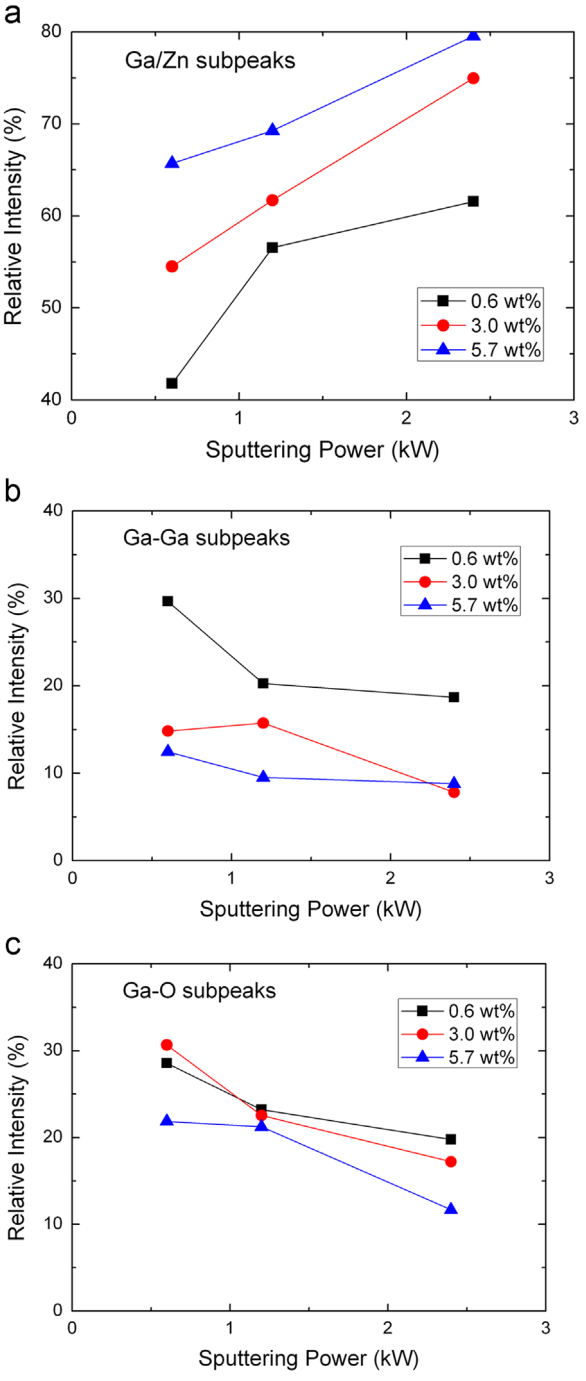

Fig. 4. Changes in the relative intensities of the subpeaks of the Ga $2p_{3/2}$ XPS peaks with varying deposition conditions.

It is now of interest in what forms these elemental Ga and oxide of Ga exist in the GZO films. Fig. 5 shows the XRD spectra obtained from the GZO samples for various deposition conditions. Except for the ZnO (0 0 2) peaks at $2\theta \approx 34.4^\circ$ common to all the XRD spectra, additional diffraction peaks appear only for the 0.6 wt% samples at $2\theta \approx 44.6^\circ$ (Fig. 5(a)–(c)). The 44.6° peaks are assigned to spinel $ZnGa_2O_4$ (4 0 0) (JCPDS 38–1240) and correlated to the relatively strong Ga–O subpeaks observed in the XPS spectra. On the other hand, the $ZnGa_2O_4$ (4 0 0) peak does not appear in 3.0 and 5.7 wt% samples (Fig. 5(d)–(i)). Absence of the oxide peak in the 3.0 and 5.7 wt% samples, despite the detection of Ga–O subpeaks in the XPS spectra, suggests that the oxide of Ga did not develop into crystalline phases in these samples. In Fig. 5, no trace of metallic Ga is observed either, while subpeaks originating from metallic Ga were detected in the XPS spectra (Fig. 3). Meanwhile, weak amorphous XRD peaks at low angles commonly appear in all the XRD spectra implying that the elemental Ga and oxide of Ga may exist in finely dispersed forms or as amorphous phase as well. It is thus suggested that the formation of impurity states near the bottom of the conduction band of the GZO films, as reflected in the absorption tails and shoulders near the absorption edges in Fig. 1, is related to the finely dispersed or amorphous metallic Ga and Ga oxide species in the GZO films.

The observations and analyses so far seem to have good correlation to the carrier concentrations shown in Table 1. It is seen that the carrier concentration in general increase with higher sputtering power and higher Ga_2O_3 concentrations in the target. In other words, higher carrier concentration is possible under the deposition conditions that suppress incorporation of metallic Ga and Ga oxide species. However, since these undesired species cannot be entirely eliminated, doping efficiency and accompanying improvement in electrical properties would be limited.

4. Conclusion

When Ga-doped ZnO films were deposited to the small thickness of 100 nm by pulsed DC magnetron sputtering at the relatively low temperature of 423 K, not all Ga supplied from the target substituted lattice Zn ions to function as dopant. Instead, substantial portion of Ga existed in the forms of metallic Ga and oxides. These non-substitutional Ga in general did not form detectable clusters or secondary phases but they seem to be related to the formation of impurity band or states that overlap with the lower part of the conduction band. Inevitably, doping efficiency as reflected in the carrier concentration were limited, although higher Ga concentration in the target and sputtering power resulted in improved doping efficiencies. Application potential of GZO as an ITO substitute would be expanded if suitable means to control the non-substitutional Ga can be found.

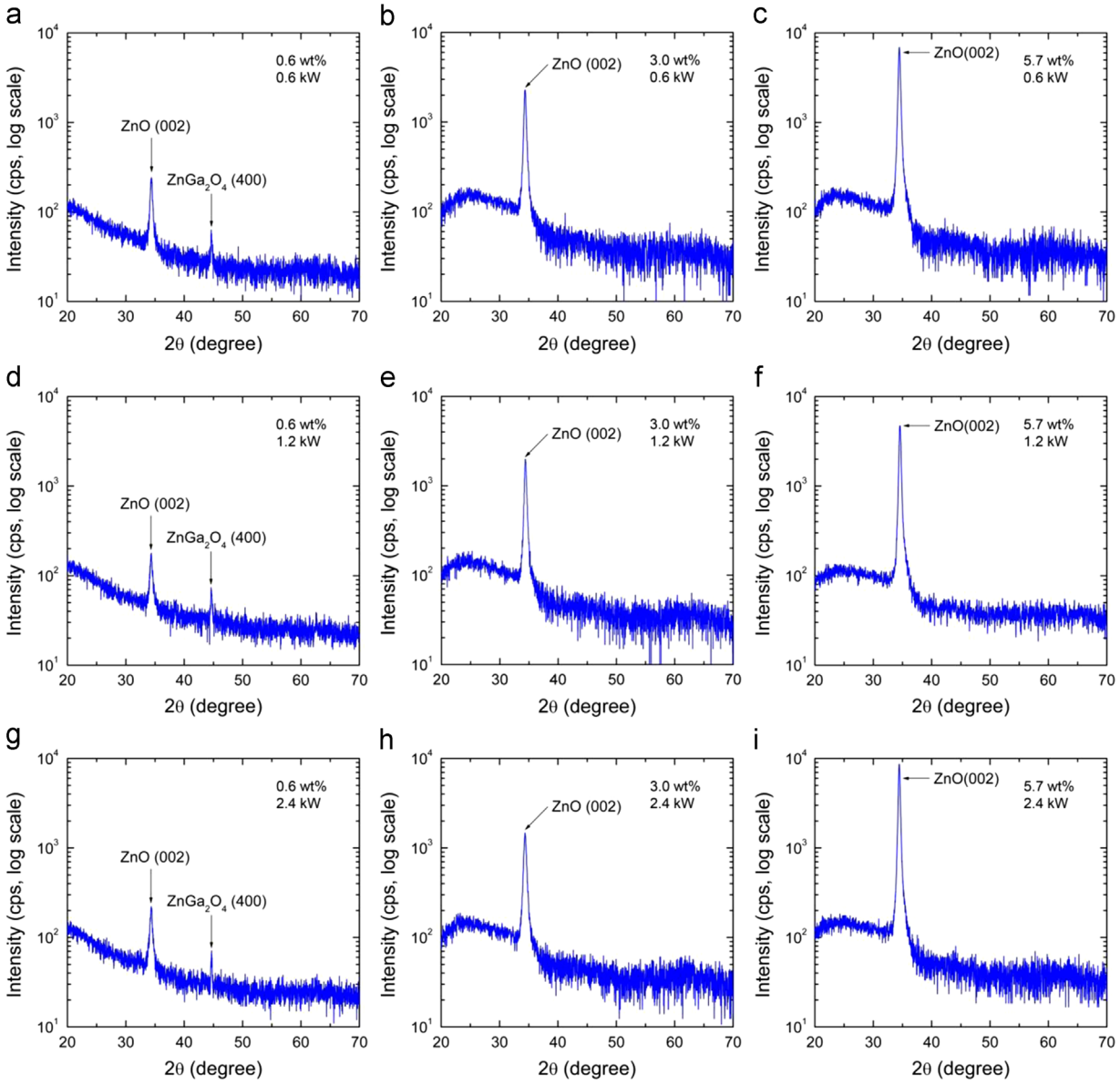

Fig. 5. XRD spectra obtained from the GZO films deposited under various deposition conditions (intensity axes are in log-scale).

Acknowledgement

This research was supported by Basic Science Research Program through the National Research Foundation (NRF) funded by the Ministry of Education, Science and Technology (2010-0006649).

References

[1] P.P. Edwards, A. Porch, M.O. Jones, D.V. Morgan, R.M. Perks, Dalton Transactions (2004) 2995–3002.
[2] T. Minami, MRS Bulletin 25 (2000) 38–44.
[3] A. Kumar, C. Zhou, ACS Nano 4 (2010) 11–14.
[4] Z. Chen, B. Cotterell, W. Wang, E. Guenther, S.A. Chua, Thin Solid Films 394 (2001) 201–205.
[5] S. Major, S. Kumar, M. Bhatnagar, K.L. Chopra, Applied Physics Letters 49 (1986) 394–396.
[6] B.G. Lewis, D.C. Paine, MRS Bulletin 25 (2000) 22–27.
[7] E. Fortunato, D. Ginley, H. Hosono, D.C. Paine, MRS Bulletin 32 (2007) 242–247.
[8] K. Ellmer, Journal of Physics D: Applied Physics 33 (2000) R17–R32.
[9] W.B. Pearson, Crystal Chemistry and Physics of Metals and Alloys, Wiley, New York, 1972.
[10] J. Vlček, A.D. Pajdarová, J. Musil, Plasma Physics 44 (2004) 426–436.
[11] J. Musil, P. Baroch, J. Vlček, K.H. Nam, J.G. Han, Thin Solid Films 475 (2005) 208–218.
[12] K. Suzuki, Thin Solid Films 351 (1999) 8–14.
[13] P.J. Kelly, R.D. Arnell, Vacuum 56 (2000) 159–172.
[14] J. O'Brien, P.J. Kelly, Surface and Coatings Technology 142–144 (2001) 621–627.
[15] E. Nam, Y.H. Kang, D. Jung, Y.S. Kim, Thin Solid Films 518 (2010) 6245–6248.

[16] S. Lee, D. Cheon, W.-J. Kim, K.-J. Ahn, W. Lee, Semiconductor Science and Technology 26 (2011) 115007.
[17] S. Lee, D. Cheon, W.-J. Kim, M.-H. Ham, W. Lee, Applied Surface Science 258 (2011) 6537–6544.
[18] J.I. Pankove, Optical Processes in Semiconductors, Dover Publications, New York, 1975.
[19] J. Tauc, R. Grigorovivi, A. Vancu, Physica Status Solidi 15 (1966) 627–637.
[20] E. Burstein, Physical Review 93 (1954) 632–633.
[21] C.L. Hinkle, M. Milojevic, B. Brennan, A.M. Sonnet, F.S. Aguirre-Tostado, G.J. Hughes, E.M. Vogel, R.M. Wallace, Applied Physics Letters 94 (2009) 162101.
[22] F. Mitsugi, Y. Umeda, N. Sakai, T. Ikegami, Thin Solid Films 518 (2010) 6334–6338.